Molecular Vision 2019; 25:780-790 <http://www.molvis.org/molvis/v25/780>
Received 25 June 2019 | Accepted 17 November 2019 | Published 19 November 2019

Expression of GluA2-containing calcium-impermeable AMPA receptors on dopaminergic amacrine cells in the mouse retina

Lei-Lei Liu, Elizabeth J. Alessio, Nathan J. Spix, Dao-Qi Zhang

Eye Research Institute, Oakland University, Rochester, MI

Purpose: The neuromodulator dopamine plays an important role in light adaptation for the visual system. Light can stimulate dopamine release from dopaminergic amacrine cells (DACs) by activating three classes of photosensitive retinal cells: rods, cones, and melanopsin-expressing intrinsically photosensitive retinal ganglion cells (ipRGCs). However, the synaptic mechanisms by which these photoreceptors excite DACs remain poorly understood. Our previous work demonstrated that α-amino-3-hydroxyl-5-methyl-4-isoxazole-propionate (AMPA) receptors contribute to light regulation of DAC activity. AMPA receptors are classified into Ca^{2+}-permeable and Ca^{2+}-impermeable subtypes. We sought to identify which subtype of AMPA receptors is involved in light regulation of DAC activity.
Methods: AMPA receptor-mediated light responses and miniature excitatory postsynaptic currents were recorded from genetically labeled DACs in mouse retinas with the whole-cell voltage-clamp mode. Immunostaining with antibodies against tyrosine hydroxylase, GluA2 (GluR2), and PSD-95 was performed in vertical retinal slices.
Results: The biophysical and pharmacological data showed that only Ca^{2+}-impermeable AMPA receptors contribute to DAC light responses driven by ipRGCs or cones (via depolarizing bipolar cells). We further found that the same subtype of AMPA receptors mediates miniature excitatory postsynaptic currents of DACs. These findings are supported by the immunohistochemical results demonstrating that DACs express the PSD-95 with GluA2, a subunit that is essential for determining the impermeability of AMPA receptors to calcium.
Conclusions: The results indicated that GluA2-containing Ca^{2+}-impermeable AMPA receptors contribute to signal transmission from photosensitive retinal cells to DACs.

Dopamine is an important neuromodulator in the central nervous system (CNS) that plays a critical role in reward, motivation, memory, attention, movement, and sensory processing [1]. During visual sensory processing, dopamine is synthesized in and released from a sparse population of retinal wide-field amacrine interneurons upon light exposure [2]. Dopamine released from these dopaminergic amacrine cells (DACs) diffuses through the cellular interstitial space of the retina and acts on numerous levels of retinal circuitry and all major classes of retinal neurons (rod and cone photoreceptors, as well as bipolar, horizontal, amacrine, and ganglion cells), mediating light adaptation for the visual system [3-8].

In response to light, DACs are excited by glutamatergic input from depolarizing (ON) bipolar cells that are driven by rod and cone photoreceptors [9-14]. DACs are also excited by the retrograde glutamatergic pathway that is initiated by the melanopsin-expressing intrinsically photosensitive retinal ganglion cells (ipRGCs) in the inner retina [11,12,15,16]. The glutamatergic inputs to DACs appear to activate postsynaptic N-methyl-D-aspartate (NMDA) receptors and α-amino-3-hydroxyl-5-methyl-4-isoxazole-propionate (AMPA) receptors, which depolarize DACs and trigger dopamine release [13,17-19].

AMPA receptors are composed of four types of subunits (GluR1–4) which determine receptor trafficking, protein interactions, and specific channel properties [20]. Of these subunits, the GluA2 (GluR2) subunit is essential in the permeability of AMPA receptors to calcium. AMPA receptors lacking GluA2 are permeable to calcium (Ca^{2+}-permeable AMPA receptors). This Ca^{2+} permeability is normally blocked by intracellular polyamines at positive membrane potentials under physiologic conditions, which results in an inwardly rectifying current-voltage (I-V) relationship for this subtype of receptors [21-23]. In contrast, GluA2-containing AMPA receptors are impermeable to calcium (Ca^{2+}-impermeable AMPA receptors), and they exhibit a linear I-V relationship [21,24].

In the retina, Ca^{2+}-permeable and Ca^{2+}-impermeable AMPA receptors are coexpressed on several types of retinal neurons, such as horizontal cells, bipolar cells, AII, and A17 amacrine cells, as well as retinal ganglion cells [25-33]. In particular, Ca^{2+}-impermeable subtypes can be converted to Ca^{2+}-permeable subtypes via activation of NMDA receptors in retinal ganglion cells [31]. In addition, Ca^{2+} influx via Ca^{2+}-permeable AMPA receptors can elicit a rapid form of postsynaptic plasticity in amacrine cells [33]. Therefore, identifying

Correspondence to: Dao-Qi Zhang, 423 Dodge Hall, 118 Library Drive, Rochester, MI 48309; Phone: (248) 370-2399; FAX: (248) 370-4211; email: zhang@oakland.edu

the subtypes of AMPA receptors expressed on DACs could provide an indication that DACs undergo synaptic plasticity during light adaptation.

We characterized biophysical and pharmacological properties of AMPA receptor-mediated light-induced responses and miniature excitatory postsynaptic currents (mEPSCs) of DACs in mouse retinas. We found that DACs express functional Ca^{2+}-impermeable AMPA receptors. This physiologic finding was supported by immunohistochemistry data demonstrating the expression of GluA2 subunits on DACs.

METHODS

Male and female adult mice (2 to 4 months old) were used for the present study. The mice were housed in the Oakland University animal facility on a 12-h:12-h light-dark cycle. Food and water were available ad libitum. All procedures conformed to National Institutes of Health (NIH) guidelines for laboratory animals and were performed in conformity with the ARVO Statement for the Use of Animals in Ophthalmic and Vision Research. The study was approved by the Institutional Animal Care and Use Committee at Oakland University.

The four mouse lines described below were used for the present study. All of the lines were bred on a mixed C57BL/129 background. The first mouse line was the wild-type mice used for the immunohistochemistry study. The second mouse line was wild-type mice in which DACs are genetically labeled by the rate-limiting enzyme catecholamine biosynthesis tyrosine hydroxylase (TH)-driven red fluorescent protein (RFP) used to visualize DACs for the mEPSC recordings (referred to as wild-type *TH*::RFP mice) [34]. The third mouse line was *TH*-RFP mice that are homozygous for the cone photoreceptor-specific cyclic nucleotide channel *Cnga3* mutation and the rod-specific G protein transducin α-subunit *Gnat1* mutation used to isolate light-induced melanopsin (*Opn4*)-based responses in DACs (*Opn4*-function-only *TH*::RFP mice) [18]. The fourth mouse line was *TH*::RFP transgenic mice homozygous for the *Gnat1* and *Opn4* mutations (cone-function-only *TH*::RFP mice) used to examine cone input to DACs [10].

Immunohistochemistry was performed as previously described [18]. Eyecups were fixed for 1 h in 4% paraformaldehyde and incubated in 30% sucrose overnight. The eyecups were frozen in a sucrose/optimum cutting temperature (OCT) solution and cut into 12 µm sections using a cryostat (Leica CM3050 S, Wetzlar, Germany). Retina slices were blocked for 2 h with 1% bovine serum albumin (BSA, Fisher Scientific, Hampton, NH) and 0.3% Triton X-100 (Sigma-Aldrich Corp., St. Louis, MO). They were then incubated overnight with primary antibodies against GluA2 (mouse monoclonal, concentration 1:500, MABN1189, or rabbit polyclonal, concentration 1:500, AB1768-I, EMD Millipore, Billerica, MA) [35,36], TH (sheep polyclonal, concentration 1:500, AB1542, EMD Millipore), and PSD-95 (mouse monoclonal, concentration 1:250, K28/43, NeuroMab, Davis, CA). Following incubation in the primary antibody, the samples were rinsed in 0.1 M PBS (1X; 137 mM NaCl, 26.8 mM KCl, 10.1 mM Na_2HPO_4, 17.6 mM KH_2PO_4, pH 7.4) and incubated in appropriate secondary antibodies (donkey anti-rabbit Alexa 488, donkey anti-sheep Alexa 568, and donkey anti-mouse Alexa 647; concentration 1:500; Life Technologies, Carlsbad, CA) for 2 h. Finally, samples were coverslipped with mounting solution (Vector Laboratories, Burlingame, CA) for imaging.

The specimens were visualized using confocal microscopy (Nikon Eclipse Ti confocal microscope, Nikon Instruments, Tokyo, Japan, or Leica TCS SP8 confocal microscope, Leica Microsystems, Wetzlar, Germany). Sequential scanning was used to eliminate crosstalk between fluorophores. All images were collected as z-stacks with 0.2 µm spacing. Images collected from the inner plexiform layer were deconvolved using NIS Elements AR. To illustrate colocalization, a single slice was selected from each image stack. NIS Elements AR was used to adjust the brightness and contrast of each channel for clarity.

Whole-cell recording procedures were identical to those described previously [18]. Briefly, an isolated retina was transferred to a recording chamber with the ganglion cell layer side up and mounted on the stage of an upright conventional fluorescence microscope (BX51WI, Olympus, Tokyo, Japan). An oxygenated extracellular medium (pH 7.4 bubbled with 95% O_2–5% CO_2) continuously perfused the recording chamber at a rate of 2–3 ml/min, and was maintained at 32–34 °C with a temperature control unit (TC-344B, Warner Instruments, Hamden, CT). The extracellular solution contained the following (in mM): 125 NaCl, 2.5 KCl, 1 $MgSO_4$, 2 $CaCl_2$, 1.25 NaH_2PO_3, 20 glucose, and 26 $NaHCO_3$. Cells and recording pipettes were viewed on a computer monitor coupled to a digital camera (XM10, Olympus, Tokyo, Japan) mounted on the microscope. After being visualized by fluorescent light using a rhodamine filter set, *TH::*RFP-expressing cells were randomly selected for recording. The identified cells and glass electrodes were then visualized using infrared differential interference contrast optics (900 nm Nomarski DIC, Olympus, Tokyo, Japan).

Whole-cell voltage-clamp recordings were made from the soma of RFP-labeled DACs using 7–10 MΩ electrodes and an Axopatch 200B amplifier (Molecular Devices,

Sunnyvale, CA). The intracellular solution for the whole-cell voltage-clamp experiments contained (in mM) 120 Cs-methanesulfonate, 5 EGTA, 10 HEPES, 5 CsCl, 5 NaCl, 0.5 $CaCl_2$, 4 Na-ATP, 0.3 Na-GTP, and 5 lidocaine n-ethyl-chloride (QX-314); the pH was adjusted to 7.2–7.4 with CsOH. QX-314 was used to block intrinsic Na^+-channel-mediated action potentials in DACs, thus highlighting extrinsic light-induced inward currents in the cells and improving the space clamp quality of the voltage clamp. TTX (1 µM) was added to block action potentials from neurons presynaptic to DACs when the DAC mEPSCs were recorded. The liquid junction potential was measured as −10 mV, and was corrected. All electrophysiological data were acquired using a Digidata 1550A digitizer (Molecular Devices, Sunnyvale, CA).

D-2-amino-5-phosphonopentanoate (D-AP5) and L-(+)-2-Amino-4-phosphonobutyric acid (L-AP4) were purchased from Hello Bio (Avonmouth, UK). All other chemicals were obtained from Tocris Bioscience (Ellisville, MO). The drugs were stored in frozen stock solutions and dissolved in an intracellular or extracellular solution before the experiments.

Light stimuli were generated using a 470-nm LED (LED Supply, Randolph, VT; and LC Corp, Brooklyn, NY) to stimulate the melanopsin chromophore (peak sensitivity of approximately 480 nm). An LED controller (Mightex, Pleasanton, CA) was used to drive the LED, and the light intensity was adjusted by varying the driving current. The light intensity was measured at the surface of the retina using an optical power meter (units were converted from µW/cm^2 to photons·cm^{-2}·s^{-1}; model 843-R; Newport, Irvine, CA). A light intensity of 4.7×10^{13} photons·cm^{-2}·s^{-1} was used for all experiments.

Electrophysiological data were analyzed using the Clampfit 10.4 (Molecular Devices), SigmaPlot 12.0 (Systat Software, San Jose, CA), and MiniAnalysis (Synaptosoft, Fort Lee, NJ) software packages. Light-induced EPSCs of the DACs were measured as the peak current evoked by the onset of the light. To assess the effects of pharmacological agents, the reduction of the light-induced peak current amplitude was evaluated for statistical significance using a paired *t* test. To construct the I-V relationship, the peak current amplitudes of AMPA receptor-mediated EPSCs recorded at −60 mV, 0 mV, and +40 mV were measured. The amplitudes at different holding potentials were normalized to the amplitude at −60 mV. Normalized peak currents from different cells at the same holding potential were averaged and then plotted against the holding potential. To quantify the rectification of the I-V relationship, the rectification index (RI) was used [31]. To calculate the RI, the predicted EPSCs' value at +40 mV was linearly extrapolated from the actual EPSCs at −60 mV to 0 mV. The RI was defined as the ratio of the actual to the predicted amplitudes of the EPSCs at +40 mV.

An analysis of the mEPSCs was conducted using Mini Analysis 6.0 (Synaptosoft) [37]. Events were automatically detected with an amplitude threshold set to twice the standard deviation of baseline noise (approximately 4 pA) from the 60-s recording of each cell. Based on the biophysical properties of the AMPA receptor-mediated events [38], the events whose 10% to 90% rise time was less than 0.1 ms or more than 10 ms were manually excluded. The amplitudes of the remaining events were pooled to construct a cumulative amplitude probability distribution using SigmaPlot. Statistical comparisons of the cumulative distributions before and during the application of a pharmacological agent were made using the Mann–Whitney U test. The amplitudes of the remaining events were also averaged to obtain the mean amplitude for each cell. The mean amplitudes of a group of cells before and during the application of a pharmacological agent were averaged, respectively, and statistical comparisons were made between them using the paired *t* test. A Student *t* test was used for comparison between two independent groups. Values are presented as the mean ± standard error of the mean (SEM) in the present study, and a p value of less than 0.05 was considered statistically significant.

RESULTS

Light-induced AMPA receptor-mediated EPSCs of DACs exhibit an outward rectification: To determine the biophysical properties of DAC AMPA receptors, we characterized the I-V relationship of AMPA receptor-mediated light-induced EPSCs of DACs. DAC light-induced EPSCs are mediated by rods, cones, and ipRGCs in the wild-type retina [9,11,15]. Because rods drive DACs through bipolar cells or AII amacrine cells that also express AMPA receptors [27,28], we genetically eliminated input from rods in the mice we used for electrophysiology. We examined inputs from cones using the cone-function-only *TH*::RFP mice and from ipRGCs using the *Opn4*-function-only *TH*::RFP mice, respectively (see the Methods section). As almost 100% of DACs receive input from ipRGCs in the dorsal retina [11], we performed DAC recordings from this region (Figure 1 and Figure 2). To isolate DAC AMPA receptor-mediated light-induced EPSCs, a cocktail of antagonists (50 µM D-AP5 for NMDA receptors, 0.3 µM ACET for Kainate receptors, 20 µM GABAzine for $GABA_A$ receptors, 50 µM TPMPA for $GABA_C$ receptors, and 1.0 µM strychnine for glycine receptors) was bath-applied to the retina. A light flash of 470 nm with a duration of 3 s and an intensity of 4.7×10^{13} photons·cm^{-2}·s^{-1} was repeatedly

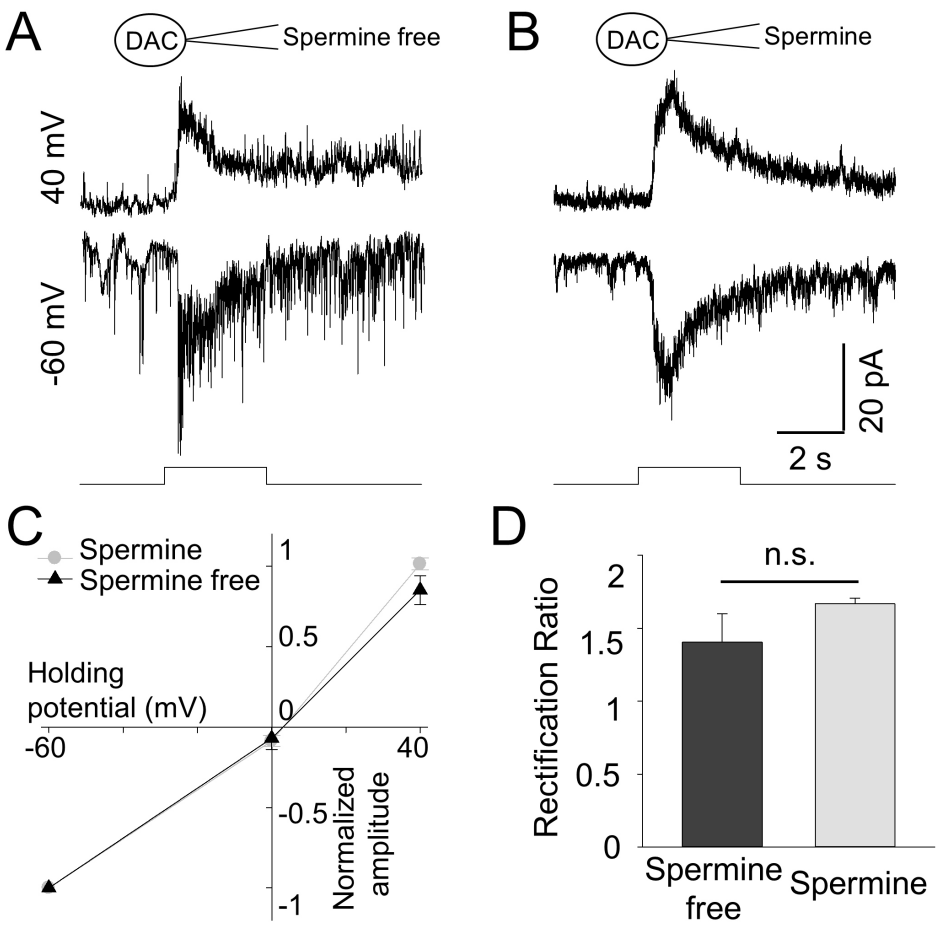

Figure 1. Biophysical properties of AMPA receptor-mediated ipRGC-driven EPSCs of DACs. α-amino-3-hydroxyl-5-methyl-4-isoxazole-propionate (AMPA) receptor-mediated light-induced excitatory postsynaptic currents (EPSCs) of dopaminergic amacrine cells (DACs) were recorded with a whole-cell patch-clamp configuration in *Opn4*-function-only flat-mount retinas at holding potentials of 40 mV and −60 mV without (**A**) and with (**B**) 100 µM spermine in the pipette solution. AMPA receptor-mediated light-induced EPSCs were isolated in the presence of a cocktail of antagonists (50 µM D-AP5 for N-methyl-D-aspartate (NMDA) receptors, 0.3 µM ACET for Kainate receptors, 20 µM GABAzine for $GABA_A$ receptors, 50 µM TPMPA for $GABA_C$ receptors, and 1.0 µM strychnine for glycine receptors). The stimulation bar shows the timing of a 470 nm light pulse (duration: 3 s; intensity: 4.7×10^{13} photons·cm^{-2}·s^{-1}). In (**C**), current-voltage relationships of AMPA receptor-mediated light-induced EPSCs from DACs including the cells in (**A**) and (**B**) were constructed (see the Methods section) without (triangles, mean ± standard error of the mean (SEM), n=4) and with (circles, mean ± SEM, n=10) spermine. The curves indicate that DAC AMPA receptor-mediated light-induced EPSCs exhibit an outward rectification, and this rectification was not changed by spermine. The rectification index (RI) of the DAC AMPA receptor-mediated light-induced EPSCs was calculated (see the Methods section), but it was not affected by spermine (**D,** mean ± SEM, n=4 for spermine free, n=10 for spermine, n.s. p>0.05, Student *t* test).

delivered to the retina every 2 min to evoke light-induced EPSCs in the DACs.

To construct an I-V curve, the DAC AMPA receptor-mediated light-induced EPSCs were measured from a DAC held at −60 mV, 0 mV, and 40 mV in the presence of the cocktail. Figure 1A illustrates an example of the AMPA receptor-mediated DAC light-induced EPSCs recorded at 40 mV and −60 mV in an *Opn4*-function-only retina. We found that the peak amplitudes of the currents at these holding voltages were close to each other (19 pA versus −23 pA). A mean I-V curve was constructed by plotting the normalized peak amplitudes of the DAC AMPA receptor-mediated light-induced EPSCs at 40 mV, 0 mV, and −60 mV (see the Methods section). Notably, the mean I-V relationship was slightly outwardly rectifying (Figure 1C).

This outwardly rectifying I-V relationship could be caused by the contribution of Ca^{2+}-impermeable AMPA receptors or disinhibition of Ca^{2+}-permeable AMPA receptors diluting the intracellular polyamines normally present in DACs. When we added the polyamine spermine (100 µM) to the recording pipette solution, however, we found that spermine did not change the I-V relationship of the DAC AMPA receptor-mediated light-induced EPSCs (Figure 1B,C). This result suggests that the contribution of Ca^{2+}-permeable AMPA receptors is limited. The conclusion is further supported by the calculation of the RI (see Methods). An RI value of 0 indicates that the light-induced EPSCs are

exclusively mediated by Ca^{2+}-permeable AMPA receptors, whereas 1 denotes exclusively Ca^{2+}-impermeable AMPA receptors [31]. The data showed that the mean value in the absence of spermine was larger than 1 (1.40±0.19, n=4). This value was not statistically significantly changed in the presence of spermine (1.67±0.04, n=10, unpaired *t* test, p>0.05, Figure 1D), indicating that the AMPA receptors that mediated the DAC light-induced EPSCs appeared to be Ca^{2+}-impermeable subtypes.

GYKI53655 but not PhTX and IEM1460 block AMPA receptor-mediated light-induced EPSCs of DACs: No specific Ca^{2+}-impermeable AMPA receptor antagonists are currently available. Therefore, we combined GYKI53655, a pan-specific AMPA receptor antagonist, and PhTX and IEM1460, two antagonists of Ca^{2+}-permeable AMPA receptors, to confirm the expression of Ca^{2+}-impermeable AMPA receptors in DACs. We found that PhTX (5 µM) had no effect on the DAC AMPA receptor-mediated light-induced EPSCs recorded from *Opn4*-function-only retinas (Figure 2A,B, control: 18.4±3.30 pA versus PhTX: 18.6±3.60 pA, n=7, paired *t* test, p>0.05). In the same mouse model, we found that IEM1460 (50 µM) had no statistically significant effect either (control: 41.25±7.930 pA versus IEM1460: 39.75±8.520 pA, n=4, paired *t* test, p>0.05). However, GYKI53655 (30 µM) almost completely blocked the DAC AMPA receptor-mediated light-induced EPSCs (Figure 2C,D, control: 27.28±3.420 pA versus GYKI: 2.57±0.68 pA, n=7, paired *t* test, p<0.001).

To determine whether input from cone photoreceptors to DACs is also mediated by Ca^{2+}-impermeable AMPA receptors, we examined DAC AMPA receptor-mediated light-induced EPSCs in the cone-function-only *TH*::RFP mice (Figure 3A, top trace). In the presence of 5 µM PhTX, the peak amplitude of the EPSCs remained unchanged (Figure 3A, bottom trace). We averaged the data obtained before and during the PhTX application, and the mean peak amplitude of the DAC AMPA receptor-mediated light-induced EPSCs was not changed by PhTX (Figure 3B, control: 11.67±2.17 pA versus PhTX: 13.63±3.690 pA, n=3, paired *t* test, p>0.05). Collectively, these results suggest that antagonists of Ca^{2+}-permeable AMPA receptors have no effect on the GYKI-sensitive AMPA receptor-mediated light-induced EPSCs of DACs, providing support for the idea that DACs express functional Ca^{2+}-impermeable AMPA receptors.

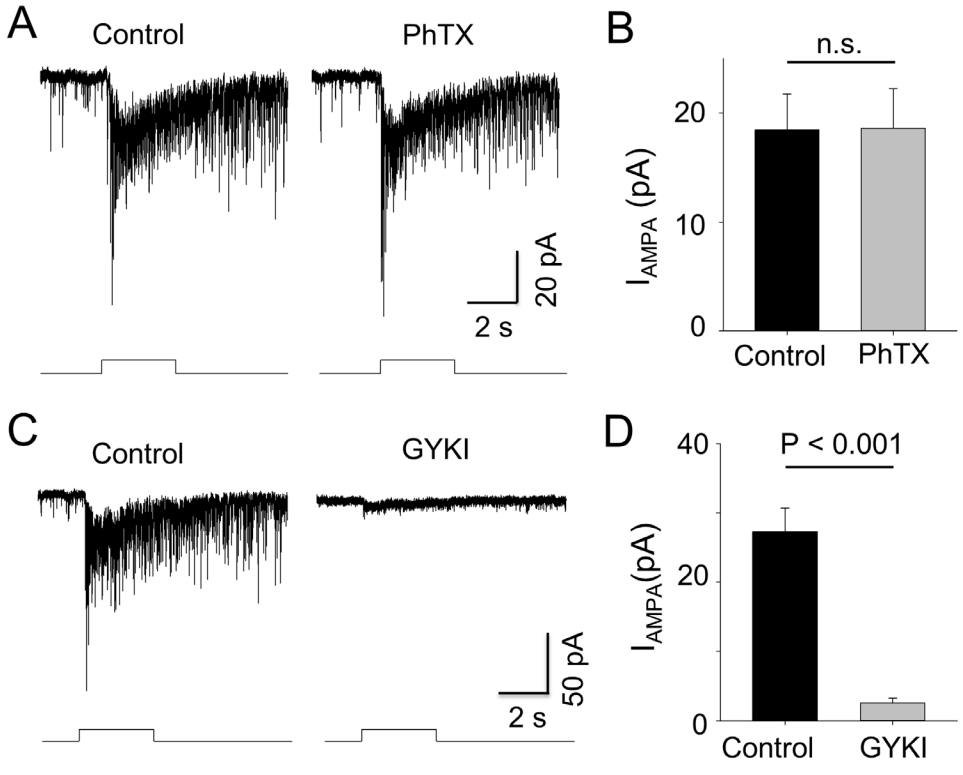

Figure 2. Ca^{2+}-impermeable AMPA receptors are involved in mediating ipRGC-driven EPSCs of DACs. The α-amino-3-hydroxyl-5-methyl-4-isoxazole-propionate (AMPA) receptor-mediated light-induced excitatory postsynaptic currents (EPSCs) of dopaminergic amacrine cells (DACs) were recorded in the presence of a cocktail of antagonists (see Figure 1) from retinas of *Opn4*-function-only *TH*::RFP mice. The DAC light-induced EPSCs were unchanged in the presence of 5 µM PhTX. A representative recording is illustrated in (**A**). Average data (mean ± standard error of the mean (SEM)) are shown in (**B**; n=7, n.s. p>0.05, paired *t* test). In contrast, 30 µM GYKI53655 almost completely blocked the DAC light-induced EPSCs (**C**). Average data (mean ± SEM) are shown in (**D**; n=7, p<0.001, paired *t* test). The DAC light-induced EPSCs stimulation bar shows the timing of a 470 nm light pulse (duration: 3 s; intensity: 4.7×10^{13} photons·cm^{-2}·s^{-1}).

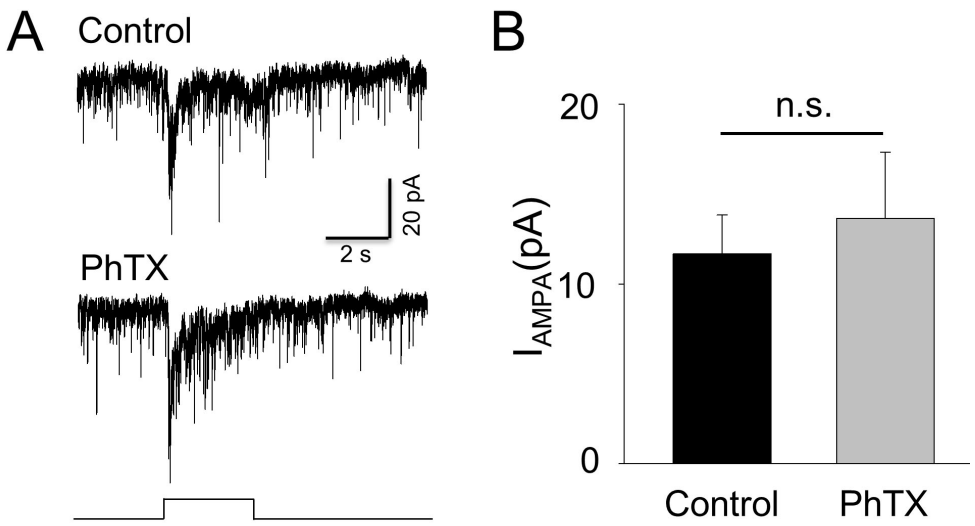

Figure 3. PhTX does not change the cone-driven AMPA receptor-mediated EPSCs of DACs. The α-amino-3-hydroxyl-5-methyl-4-isoxazole-propionate (AMPA) receptor-mediated light-induced excitatory postsynaptic currents (EPSCs) of dopaminergic amacrine cells (DACs) were recorded in the presence of a cocktail of antagonists (see Figure 1) from retinas of cone-function-only *TH*::RFP mice. The DAC light-induced EPSCs were unchanged in the presence of 5 µM PhTX. A representative recording is illustrated in (**A**). Average data (mean ± standard error of the mean (SEM)) are shown in (**B**; n=3, n.s. p>0.05, paired *t* test). The data suggest that the AMPA receptors that mediate cone-driven DAC light responses are unlikely Ca^{2+}-permeable subtypes.

PhTX does not change the amplitude of AMPA receptor-mediated mEPSCs of DACs: We next determined whether PhTX affects the amplitude of the DAC AMPA receptor-mediated mEPSCs, which are generated by the spontaneous release of a single vesicle or quantum of glutamate onto a postsynaptic neuron in the absence of presynaptic action potentials. Changes in mEPSC amplitude generally reflect postsynaptic modulation, whereas changes in mEPSC frequency are associated with presynaptic changes in the probability of quantal release [39]. To eliminate action potentials, 1 µM TTX was added to the cocktail of antagonists described above. An examination of whole-cell voltage-clamp recordings from the DACs in wild-type *TH::*RFP retinas at the holding potential of −70 mV revealed events resembling mEPSCs (Figure 4A, top trace). These events could be mediated by glutamatergic input from ON-bipolar cells, ipRGCs, or both. The events were completely blocked by 50 µM GYKI53655 (data not shown), suggesting that DAC mEPSCs are mediated by AMPA receptors. However, 5 µM PhTX had no notable effect on the DAC mEPSCs (Figure 4A, bottom trace). Cumulative probability distributions of AMPA receptor-mediated mEPSC amplitudes were constructed and compared before and during the application of PhTX for each DAC tested (n=6). PhTX did not statistically significantly alter the amplitude probability distributions in each tested DAC (Figure 4B, Mann–Whitney U test, p>0.05). We also averaged the AMPA receptor-mediated mEPSC amplitudes before and during the application of PhTX from six DACs, and the mean amplitude was not changed by PhTX (Figure 4C). The results further support the notion that DACs express functional Ca^{2+}-impermeable AMPA receptors.

Expression of GluA2 subunits on the processes of DACs: To further validate the DACs' exhibition of Ca^{2+}-impermeable AMPA receptors, we examined the expression of GluA2 subunits on DACs using immunohistochemistry. We colabeled GluA2 and TH in vertical retinal slices of the wild-type mice. Mouse monoclonal and rabbit polyclonal antibodies against GluA2 were used [35,36]. For the mouse monoclonal antibody, we found that dense punctate GluA2 staining was observed in the inner plexiform layer (Figure 5, middle panel). Within this layer, putative colocalization of GluA2 and TH was detected in the processes of the TH-labeled cells (Figure 5, right panel).

For the rabbit polyclonal antibody, we found that dense GluA2-immunoreactive puncta were distributed in the inner nuclear layer and the inner plexiform layer (Figure 6A2, green). To determine whether the punctate GluA2 staining on TH-positive processes (Figure 6A1, red) coexpresses with synaptic proteins, we included PSD-95, a post-synaptic protein marker in the staining. Dense PSD-95-immunoreactive puncta were observed in the inner plexiform layer (Figure 6A3, blue). Some overlapped with GluA2 staining on the TH-positive processes (Figure 6A4, arrows), but others did not (Figure 6A4, open arrowheads). PSD-95 non- colocalized GluA2 puncta (Figure 6A4, arrowheads) were also observed on the TH-positive processes. Two additional overlay images (Figure 6B,C) revealed more colocalizations of PSD-95 and GluA2 staining on TH-positive processes. The results suggest

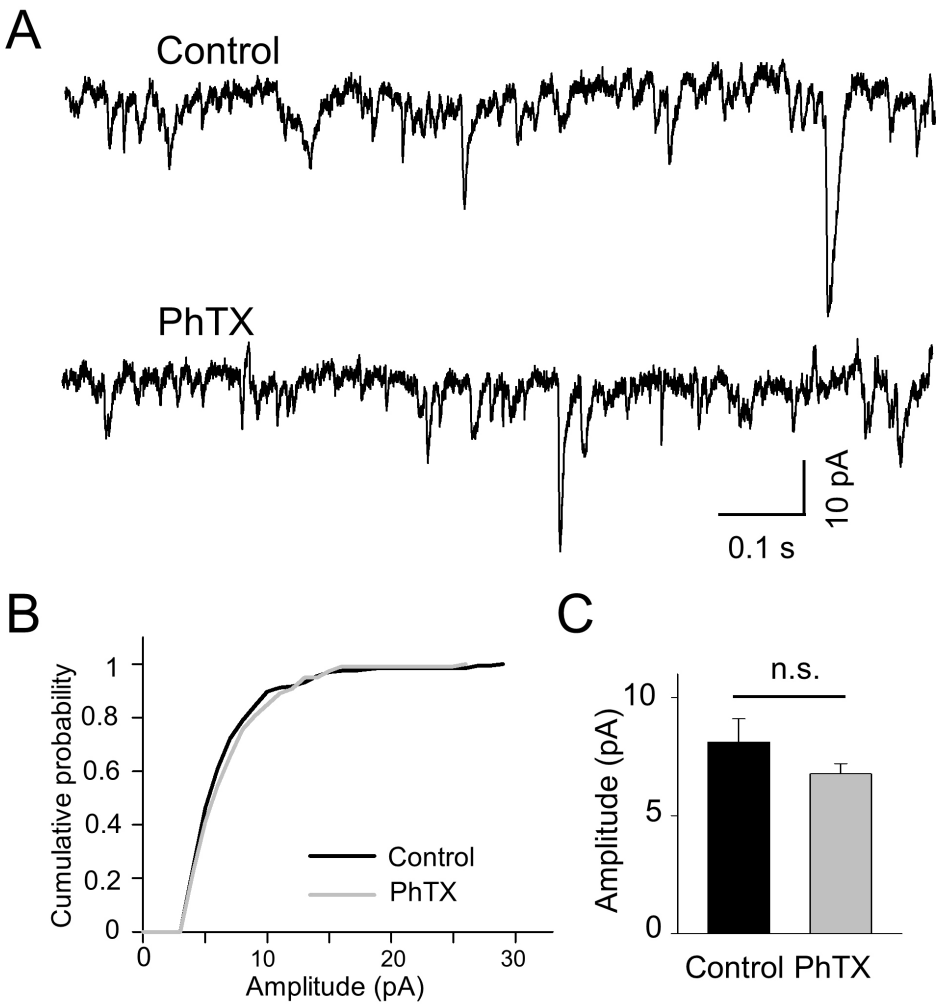

Figure 4. Ca^{2+}-permeable AMPA receptors are unlikely involved in mediating DAC miniature EPSCs (mEPSCs). α-amino-3-hydroxyl-5-methyl-4-isoxazole-propionate (AMPA) receptor-mediated miniature excitatory postsynaptic currents (mEPSCs) were recorded from dopaminergic amacrine cells (DACs) in wild-type *TH*::RFP mice at the holding potential of −70 mV in the presence of 1 µM TTX and a cocktail of antagonists (see Figure 1). **A**: Representative sweeps recorded from a DAC before and during 5 µM PhTX are shown. **B**: Cumulative probability distributions of AMPA receptor-mediated mEPSC amplitudes from this cell show that PhTX had no effect ($p>0.05$, Mann–Whitney U test). **C**: A bar graph shows that average AMPA receptor-mediated mEPSC amplitudes were not changed by PhTX (mean ± standard error of the mean (SEM), n=6, $p>0.05$, paired *t* test).

that putative synaptic and extrasynaptic GluA2-containing AMPA receptors are expressed on DACs. Similar results were observed in retinas obtained from three additional mice.

DISCUSSION

The major finding of the present study is that GluA2-containing Ca^{2+}-impermeable AMPA receptors contribute to signal transmission from photosensitive retinal cells to DACs. First, the Ca^{2+}-permeable AMPA receptor antagonist PhTX had no detectable effects on DAC AMPA receptor-mediated light-evoked EPSCs and mEPSCs, supporting the idea that DACs express functional Ca^{2+}-impermeable AMPA receptors. We noticed that PhTX-resistant Ca^{2+}-permeable AMPA receptors are expressed on retinal neurons [40]. These neurons are highly unlikely to be DACs, because of the consistent results obtained by two additional Ca^{2+}-permeable AMPA receptor antagonists: IEM1460 and spermine. Second, the I-V relationship of the DAC AMPA receptor-mediated light-evoked EPSCs showed an outward rectification. This outwardly rectifying I-V relationship was exactly the opposite of the inwardly rectifying I-V relationship of Ca^{2+}-permeable AMPA receptors, further demonstrating that DACs express GluA2-containing Ca^{2+}-impermeable AMPA receptors. Finally, GluA2 subunits were coexpressed with PSD-95 on the processes of DACs. This result expands our previous finding that DACs express AMPA receptors with a pan-AMPA receptor antibody by demonstrating a specific subunit on this cell type [17]. Although these DACs were not the cells used to perform electrophysiology, the data implied that CluA2-containing Ca^{2+}-impermeable AMPA receptors contribute to signal transmission from photosensitive cells to DACs in the mouse retina.

Observing that AMPA receptors show an outwardly rectifying I-V relationship is unusual. A previous study demonstrated that somatic outside-out patches that express

extrasynaptic Ca^{2+}-impermeable AMPA receptors exhibit an outwardly rectifying I-V relationship [41]. Dense punctate GluA2 immunostaining with a rabbit polyclonal antibody was observed in the inner nuclear layer where somata are located. PSD-95 non-colocalized GluA2 puncta were also seen in TH positive processes. These results suggest that DACs may express extrasynaptic GluA2-contained AMPA receptors, contributing to the outwardly rectifying I-V relationship of DAC AMPA receptors. In contrast to the rabbit polyclonal GluA2 antibody, the mouse monoclonal GluA2 immunoreactive puncta were primarily distributed in the inner plexiform layer. The cause of this difference is unclear [35,36]. As the PSD-95 antibody used was also raised in mice, we were unable to use the mouse monoclonal GluA2 antibody to demonstrate the extrasynaptic expression of GluA2 on DACs. Therefore, the extent to which the outwardly rectifying I-V relationship of DAC AMPA receptors is a result of their extrasynaptic expression remains to be further investigated.

The present results suggest that GluA2-containing Ca^{2+}-impermeable AMPA receptors contribute to the direct glutamatergic inputs from ON cone bipolar cells and ipRGCs to DACs, but the GluA2-lacking Ca^{2+}-permeable AMPA receptors do not [17]. ON cone bipolar cells can relay cone signals directly to DACs. Rod signals also enter ON cone bipolar cells through the primary rod pathway (rod → rod bipolar cell → AII amacrine cell → cone bipolar cell) and then enter the DACs. In this rod pathway, AII amacrine cells contain Ca^{2+}-permeable and Ca^{2+}-impermeable AMPA receptors [28]. Therefore, Ca^{2+}-permeable AMPA receptors on AII amacrine cells are also involved in signal transmission from rods to DACs through ON cone bipolar cells.

Research to date has demonstrated that AMPA and NMDA receptors are coexpressed on DAC synapses, mediating dopamine release during light adaptation [13,17-19]. The present results imply that Ca^{2+}-impermeable AMPA receptors mediate fast signal transmission to DACs. Because NMDA receptors are Ca^{2+}-permeable [42], they could mediate the synaptic plasticity of the dopaminergic network during light adaptation. NMDA receptor-induced synaptic plasticity of AMPA receptors is the best-understood mechanism for activity-dependent regulation of synaptic strength, such as short- and long-term potentiation in the CNS [43,44]. In the retina, light can convert Ca^{2+}-impermeable AMPA receptors to Ca^{2+}-permeable AMPA receptors in retinal ganglion cells by activation of NMDA receptors [31]. If this also occurs on DACs, the activation of NMDA receptors could result in the conversion of Ca^{2+}-impermeable AMPA receptors to Ca^{2+}-permeable AMPA receptors. The newly inducted Ca^{2+}-permeable AMPA receptors have a high Ca^{2+} permeability, which could provide an additional source of intracellular Ca^{2+}. This process enhances further AMPA receptor insertion, promoting metaplasticity and facilitating NMDA receptor-mediated potentiation of signal transmission to DACs.

ACKNOWLEDGMENTS

We thank Douglas McMahon and Samer Hattar for kindly providing transgenic mice for our research. This work was supported by NIH grants R01EY022640 (D-QZ), the Alliance

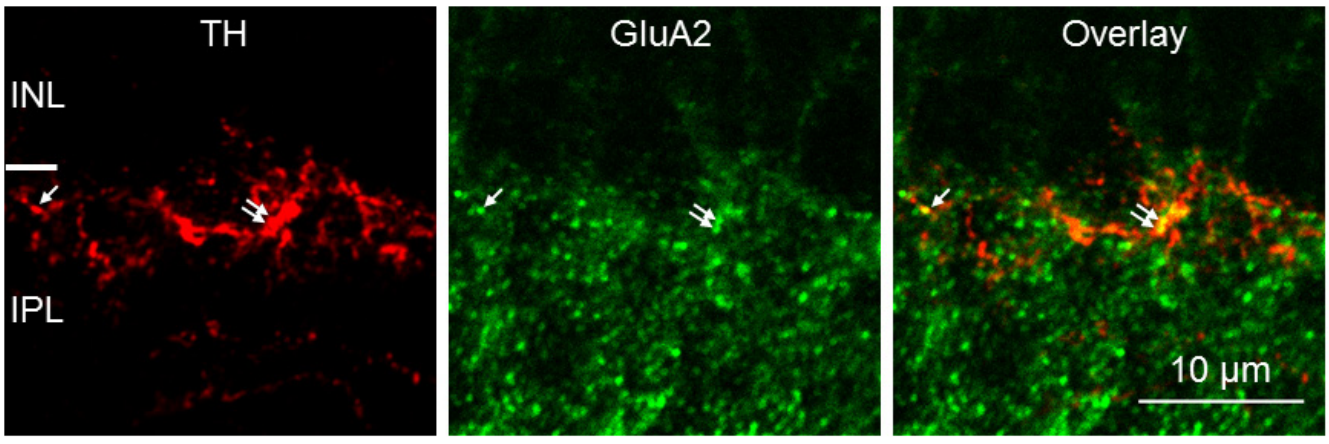

Figure 5. GluA2 subunits are expressed on TH-positive processes. Double immunostaining experiments using antibodies against TH and GluA2 (a mouse monoclonal antibody) were performed in wild-type mouse retinal vertical slices. A single optical section (0.2 µm thickness) shows colocalization of GluA2 and TH staining. Left (red), TH-positive cell processes in the IPL. Middle (green), dense punctate expression of GluA2 in the IPL and sparse expression in the INL. Right, merged image demonstrating putative colocalization (arrows) of TH and GluA2 on TH-positive processes. INL, inner nuclear layer; IPL, inner plexiform layer. Similar results were obtained from three additional mice.

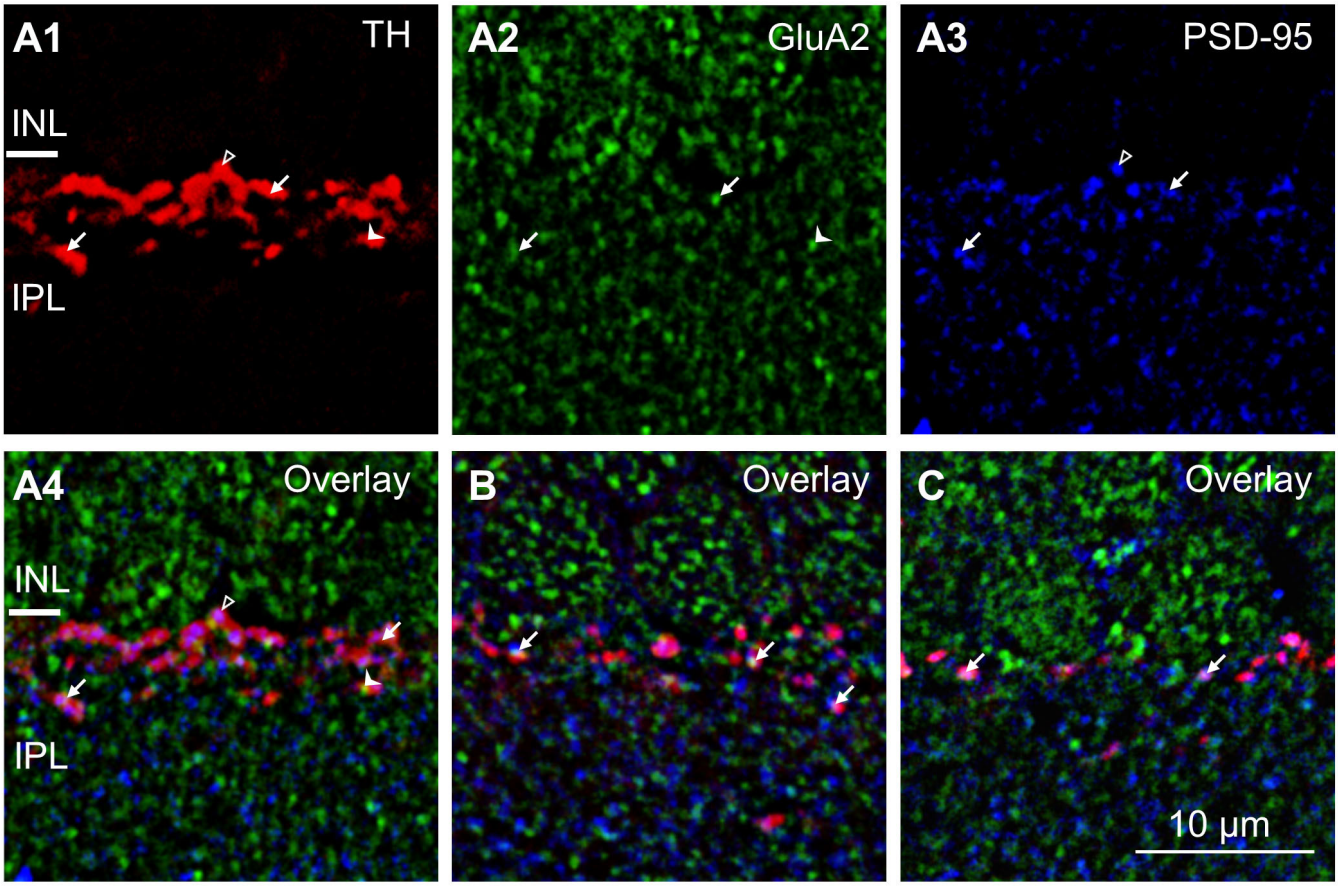

Figure 6. Expression of GluA2 and PSD-95 on the processes of DACs. Triple immunostaining experiments using antibodies against TH, PSD-95, and GluA2 (rabbit polyclonal antibodies) were performed in wild-type mouse retinal vertical slices. A single optical section (0.2 µm thickness) shows colocalization of GluA2 and PSD-95 staining on TH positive processes. **A1**: DAC processes labeled with TH (red). **A2**: GluA2 puncta (green). **A3**: PSD-95 puncta (blue). **A4**: Overlay. Arrows indicate points of triple-colocalization, showing colocalization of GluA2 and PSD-95 in the DAC processes. The arrowheads show colocalization of TH and GluA2 in the absence of PSD-95. The open arrowheads point to colocalizations of TH and PSD-95 in the absence of GluA2. **B** and **C**: Overlay images demonstrate colocalizations of TH, PSD-95, and GluA2 staining (arrows). INL, inner nuclear layer; IPL, inner plexiform layer. Similar results were obtained from three additional mice. Scale bar: 10 µm.

for Vision Research Award (L-LL), and the Wayne State Vision Core P30EY004068.

REFERENCES

1. Klein MO, Battagello DS, Cardoso AR, Hauser DN, Bittencourt JC, Correa RG. Dopamine: Functions, Signaling, and Association with Neurological Diseases. Cell Mol Neurobiol 2019; 39:31-59. [PMID: 30446950].

2. Witkovsky P. Dopamine and retinal function. Doc Ophthalmol 2004; 108:17-40. [PMID: 15104164].

3. Mills SL, Xia XB, Hoshi H, Firth SI, Rice ME, Frishman LJ, Marshak DW. Dopaminergic modulation of tracer coupling in a ganglion-amacrine cell network. Vis Neurosci 2007; 24:593-608. [PMID: 17711603].

4. Lasater EM, Dowling JE. Dopamine decreases conductance of the electrical junctions between cultured retinal horizontal cells. Proc Natl Acad Sci USA 1985; 82:3025-9. [PMID: 3857632].

5. Jackson CR, Ruan GX, Aseem F, Abey J, Gamble K, Stanwood G, Palmiter RD, Iuvone PM, McMahon DG. Retinal dopamine mediates multiple dimensions of light-adapted vision. J Neurosci 2012; 32:9359-68. [PMID: 22764243].

6. Jackson CR, Chaurasia SS, Hwang CK, Iuvone PM. Dopamine D(4) receptor activation controls circadian timing of the adenylyl cyclase 1/cyclic AMP signaling system in mouse retina. Eur J Neurosci 2011; 34:57-64. [PMID: 21676039].

7. Ichinose T, Lukasiewicz PD. Ambient light regulates sodium channel activity to dynamically control retinal signaling. J Neurosci 2007; 27:4756-64. [PMID: 17460088].

8. Vaquero CF, Pignatelli A, Partida GJ, Ishida AT. A dopamine- and protein kinase A-dependent mechanism for network adaptation in retinal ganglion cells. J Neurosci 2001; 21:8624-35. [PMID: 11606650].

9. Zhang DQ, Zhou TR, McMahon DG. Functional heterogeneity of retinal dopaminergic neurons underlying their multiple roles in vision. J Neurosci 2007; 27:692-9. [PMID: 17234601].

10. Qiao SN, Zhang Z, Ribelayga CP, Zhong YM, Zhang DQ. Multiple cone pathways are involved in photic regulation of retinal dopamine. Sci Rep 2016; 6:28916-[PMID: 27356880].

11. Zhao X, Wong KY, Zhang DQ. Mapping physiological inputs from multiple photoreceptor systems to dopaminergic amacrine cells in the mouse retina. Sci Rep 2017; 7:7920-[PMID: 28801634].

12. Newkirk GS, Hoon M, Wong RO, Detwiler PB. Inhibitory inputs tune the light response properties of dopaminergic amacrine cells in mouse retina. J Neurophysiol 2013; 110:536-52. [PMID: 23636722].

13. Perez-Fernandez V, Milosavljevic N, Allen AE, Vessey KA, Jobling AI, Fletcher EL, Breen PP, Morley JW, Cameron MA. Rod Photoreceptor Activation Alone Defines the Release of Dopamine in the Retina. Current biology: CB 2019; 29(5):763–74 e5.

14. Dumitrescu ON, Pucci FG, Wong KY, Berson DM. Ectopic retinal ON bipolar cell synapses in the OFF inner plexiform layer: contacts with dopaminergic amacrine cells and melanopsin ganglion cells. J Comp Neurol 2009; 517:226-44. [PMID: 19731338].

15. Zhang DQ, Wong KY, Sollars PJ, Berson DM, Pickard GE, McMahon DG. Intraretinal signaling by ganglion cell photoreceptors to dopaminergic amacrine neurons. Proc Natl Acad Sci USA 2008; 105:14181-6. [PMID: 18779590].

16. Atkinson CL, Feng J, Zhang DQ. Functional integrity and modification of retinal dopaminergic neurons in the rd1 mutant mouse: roles of melanopsin and GABA. J Neurophysiol 2013; 109:1589-99. [PMID: 23255724].

17. Zhang DQ, Belenky MA, Sollars PJ, Pickard GE, McMahon DG. Melanopsin mediates retrograde visual signaling in the retina. PLoS One 2012; 7:e42647-[PMID: 22880066].

18. Liu LL, Spix NJ, Zhang DQ. NMDA Receptors Contribute to Retrograde Synaptic Transmission from Ganglion Cell Photoreceptors to Dopaminergic Amacrine Cells. Front Cell Neurosci 2017; 11:279-[PMID: 28959188].

19. Prigge CL, Yeh PT, Liou NF, Lee CC, You SF, Liu LL, McNeill DS, Chew KS, Hattar S, Chen SK, Zhang DQ. M1 ipRGCs Influence Visual Function through Retrograde Signaling in the Retina. J Neurosci 2016; 36:7184-97. [PMID: 27383593].

20. Jacobi E, von Engelhardt J. Diversity in AMPA receptor complexes in the brain. Curr Opin Neurobiol 2017; 45:32-8. [PMID: 28376410].

21. Bowie D, Mayer ML. Inward rectification of both AMPA and kainate subtype glutamate receptors generated by polyamine-mediated ion channel block. Neuron 1995; 15:453-62. [PMID: 7646897].

22. Swanson GT, Kamboj SK, Cull-Candy SG. Single-channel properties of recombinant AMPA receptors depend on RNA editing, splice variation, and subunit composition. J Neurosci 1997; 17:58-69. [PMID: 8987736].

23. Washburn MS, Numberger M, Zhang S, Dingledine R. Differential dependence on GluR2 expression of three characteristic features of AMPA receptors. J Neurosci 1997; 17:9393-406. [PMID: 9390995].

24. Cull-Candy S, Kelly L, Farrant M. Regulation of Ca2+-permeable AMPA receptors: synaptic plasticity and beyond. Curr Opin Neurobiol 2006; 16:288-97. [PMID: 16713244].

25. Okada T, Schultz K, Geurtz W, Hatt H, Weiler R. AMPA-preferring receptors with high Ca2+ permeability mediate dendritic plasticity of retinal horizontal cells. Eur J Neurosci 1999; 11:1085-95. [PMID: 10103101].

26. Huang SY, Liang PJ. Ca2+-permeable and Ca2+-impermeable AMPA receptors coexist on horizontal cells. Neuroreport 2005; 16:263-6. [PMID: 15706232].

27. Gilbertson TA, Scobey R, Wilson M. Permeation of calcium ions through non-NMDA glutamate channels in retinal bipolar cells. Science 1991; 251:1613-5. [PMID: 1849316].

28. Morkve SH, Veruki ML, Hartveit E. Functional characteristics of non-NMDA-type ionotropic glutamate receptor channels in AII amacrine cells in rat retina. J Physiol 2002; 542:147-65. [PMID: 12096058].

29. Singer JH, Diamond JS. Sustained Ca2+ entry elicits transient postsynaptic currents at a retinal ribbon synapse. J Neurosci 2003; 23:10923-33. [PMID: 14645488].

30. Chavez AE, Singer JH, Diamond JS. Fast neurotransmitter release triggered by Ca influx through AMPA-type glutamate receptors. Nature 2006; 443:705-8. [PMID: 17036006].

31. Jones RS, Carroll RC, Nawy S. Light-induced plasticity of synaptic AMPA receptor composition in retinal ganglion cells. Neuron 2012; 75:467-78. [PMID: 22884330].

32. Casimiro TM, Nawy S, Carroll RC. Molecular mechanisms underlying activity-dependent AMPA receptor cycling in retinal ganglion cells. Mol Cell Neurosci 2013; 56:384-92. [PMID: 23911793].

33. Kim MH, von Gersdorff H. Postsynaptic Plasticity Triggered by Ca(2)(+)-Permeable AMPA Receptor Activation in Retinal Amacrine Cells. Neuron 2016; 89:507-20. [PMID: 26804991].

34. Zhang DQ, Stone JF, Zhou T, Ohta H, McMahon DG. Characterization of genetically labeled catecholamine neurons in the mouse retina. Neuroreport 2004; 15:1761-5. [PMID: 15257143].

35. Gustafson EC, Morgans CW, Tekmen M, Sullivan SJ, Esguerra M, Konno R, Miller RF. Retinal NMDA receptor function and expression are altered in a mouse lacking D-amino acid oxidase. J Neurophysiol 2013; 110:2718-26. [PMID: 24068757].

36. Haverkamp S, Grunert U, Wassle H. The synaptic architecture of AMPA receptors at the cone pedicle of the primate retina. J Neurosci 2001; 21:2488-500. [PMID: 11264323].

37. Feigenspan A, Babai N. Functional properties of spontaneous excitatory currents and encoding of light/dark transitions in horizontal cells of the mouse retina. Eur J Neurosci 2015; 42:2615-32. [PMID: 26173960].

38. Alberto CO, Hirasawa M. AMPA receptor-mediated miniature EPSCs have heterogeneous time courses in orexin neurons. Biochem Biophys Res Commun 2010; 400:707-12. [PMID: 20816937].

39. Cormier RJ, Kelly PT. Glutamate-induced long-term potentiation enhances spontaneous EPSC amplitude but not frequency. J Neurophysiol 1996; 75:1909-18. [PMID: 8734590].

40. Osswald IK, Galan A, Bowie D. Light triggers expression of philanthotoxin-insensitive Ca2+-permeable AMPA receptors in the developing rat retina. J Physiol 2007; 582:95-111. [PMID: 17430992].

41. Liu SQ, Cull-Candy SG. Synaptic activity at calcium-permeable AMPA receptors induces a switch in receptor subtype. Nature 2000; 405:454-8. [PMID: 10839540].

42. Hansen KB, Yi F, Perszyk RE, Furukawa H, Wollmuth LP, Gibb AJ, Traynelis SF. Structure, function, and allosteric modulation of NMDA receptors. J Gen Physiol 2018; 150:1081-105. [PMID: 30037851].

43. Derkach VA, Oh MC, Guire ES, Soderling TR. Regulatory mechanisms of AMPA receptors in synaptic plasticity. Nat Rev Neurosci 2007; 8:101-13. [PMID: 17237803].

44. Rao VR, Finkbeiner S. NMDA and AMPA receptors: old channels, new tricks. Trends Neurosci 2007; 30:284-91. [PMID: 17418904].

Articles are provided courtesy of Emory University and the Zhongshan Ophthalmic Center, Sun Yat-sen University, P.R. China. The print version of this article was created on 19 November 2019. This reflects all typographical corrections and errata to the article through that date. Details of any changes may be found in the online version of the article.